Optically detected magnetic resonance of group-IV and group-VI impurities in AlAs and $Al_xGa_{1-x}As$ with $x \geq 0.35$

E. R. Glaser, T. A. Kennedy, B. Molnar, and R. S. Sillmon
Naval Research Laboratory, Washington, D.C. 20375

M. G. Spencer
Department of Electrical Engineering, Howard University, Washington, D.C. 20059

M. Mizuta
Fundamental Research Laboratory, NEC Corporation, 34 Miyukigaoka, Tsukuba 305, Japan

T. F. Kuech*
IBM Research Division, Thomas J. Watson Research Center, P. O. Box 218, Yorktown Heights, New York 10598
(Received 11 February 1991)

Optically detected magnetic-resonance (ODMR) experiments have been performed on *n*-doped epitaxial layers of AlAs and $Al_xGa_{1-x}As$ with $x \geq 0.35$ grown on (001) GaAs substrates. The $Al_xGa_{1-x}As$ layers were doped during growth or via implantation with Si and Sn impurities from group IV and S, Se, and Te impurities from group VI. The studies were carried out with the as-grown layers on the parent GaAs substrates, removed from the substrates, and attached to substrates with larger lattice constants at low temperatures. Symmetry information was obtained from angular-rotation studies with the magnetic field rotated in the $(1\bar{1}0)$ and (001) crystal planes. Also, uniaxial stress along the $[1\bar{1}0]$ and [100] directions has been combined with ODMR to further probe the symmetry of the donor states. The magnetic resonance was detected mainly on deep (1.0–1.8 μm) radiative-recombination processes. The donor state in Si-doped AlAs can be described by the usual hydrogenic effective-mass theory for substitutional donors on the group-III site associated with the *X*-point conduction-band minima. The *g*-value anisotropy and splitting observed from the rotation studies in the $(1\bar{1}0)$ and (001) planes, respectively, can be understood using an independent-valley model. The Si-donor *g* values in AlAs are the following: $g_\perp = 1.976 \pm 0.001$ and $g_\parallel = 1.917 \pm 0.001$ with respect to the long axes of the *X*-valley ellipsoid. The results obtained for the $Al_xGa_{1-x}As$ layers doped with S, Se, and Te, particularly for samples with $x \geq 0.6$, can be described by the hydrogenic effective-mass theory modified by a finite valley-orbit (i.e., central cell) interaction that mixes the states derived from the X_x, X_y, and X_z valleys to form an A_1 ground state, as predicted by Morgan. Analyses of these results within the virtual-crystal approximation yield valley-orbit splitting energies (i.e., chemical shifts) of ~16–20 meV for these group-VI donors in $Al_{0.6}Ga_{0.4}As$. The nature of the donor states in the Si-doped $Al_xGa_{1-x}As$ heterostructures with $x < 1$ is more complicated. The monotonic decrease in both the *g*-value anisotropy and splitting with decreasing Al mole fraction and the increase in the linewidth of the donor resonances from 7 mT for AlAs:Si to 14 mT for $Al_{0.4}Ga_{0.6}As$:Si indicate a breakdown of the independent-valley model employed to describe the symmetry of the donor ground state in Si-doped AlAs. Various mechanisms that can potentially influence the properties of the donor ground state in Si-doped $Al_xGa_{1-x}As$ with $x < 1$, such as a finite spin-valley interaction, *L*-*X* (or Γ-*X*) interband mixing, and alloy disorder, are discussed. The results for the Sn-doped AlAs and $Al_xGa_{1-x}As$/GaAs heterostructures provide evidence that the optically active states revealed in these studies are much deeper compared to the Si donor states.

I. INTRODUCTION

Over the past few years much attention has been given to the doping of $Al_xGa_{1-x}As$ crystals with group-IV or group-VI impurity atoms. A variety of experiments and theoretical treatments have shown that such doping can result in the formation of both shallow and deep levels.[1] The nature of these levels is of utmost practical interest since they control the electrical and optical properties of this technologically important material. It is generally accepted that these levels are associated with the same defect, the *DX* center. The phenomenon of persistent photoconductivity at low temperatures observed strongly in $Al_xGa_{1-x}As$ with $0.22 \leq x \leq 0.42$ is associated with the existence of the deep level. However, the microscopic structure and charge state of the *DX* center in the relaxed configuration are subjects of considerable debate. Recently, electron paramagnetic-resonance (EPR) experi-

ments have been carried out on n-doped $Al_xGa_{1-x}As$ crystals by a number of groups to address the issue of the charge state of the DX center.[2–4] The nonobservation of a resonance at low temperatures and under dark conditions is thought to be consistent with a negative-U model for the DX center.[5] However, the paramagnetism detected in magnetic susceptibility experiments carried out under similar conditions strongly challenges this model.[6]

Magnetic-resonance experiments have been most successful in revealing the nature of the shallow, metastable state associated with the X-point conduction-band minima in n-doped $Al_xGa_{1-x}As$ with $x \geq 0.35$. Early EPR studies[7] on bulk single crystals of $Al_xGa_{1-x}As$ ($0.64 \leq x \leq 0.84$) grown from a Ga solution detected a line with $g \sim 1.95$ ascribed to the X-related shallow level. The spectrum was assigned to residual Si donors since the carrier concentration correlated with the amplitude of the EPR signal. These studies were extended to 100-μm-thick $Al_xGa_{1-x}As$ layers ($0.55 \leq x \leq 0.8$) grown on GaAs substrates by liquid-phase epitaxy (LPE).[7] The donor resonance was found to be anisotropic in the $(1\bar{1}0)$ plane in these samples.

During the past three years, extensive optically detected magnetic-resonance (ODMR) experiments performed on much thinner (1–7 μm) Si-doped AlAs and $Al_xGa_{1-x}As$ layers, with $x \geq 0.35$, on (001) GaAs by our group[8,9,10] and workers at Philips Laboratories[11–13] have found a resonance with similar g values and anisotropic behavior as observed in the previous EPR experiments.[7] In addition, the full symmetry of the shallow state was revealed from angular-rotation studies in both the $(1\bar{1}0)$ and (001) planes of these samples.[14] The (001) results were independently verified by EPR experiments[15] and more recent ODMR experiments by the Philips group[13] on similar samples. Also, the results of ODMR studies carried out to examine the influence of the chemically different donor species S, Se, and Si on the nature of shallow donor states in $Al_{0.6}Ga_{0.4}As$/GaAs heterostructures have been preliminarily reported.[16] EPR studies have also been recently performed on Te-doped[17] and Sn-doped[2] $Al_xGa_{1-x}As$ epitaxial layers with $x = 0.3$.

The present work provides a comprehensive report of recent optically detected magnetic-resonance experiments performed on n-doped epitaxial layers of AlAs and $Al_xGa_{1-x}As$ ($x \geq 0.35$) grown on (001) GaAs substrates. The $Al_xGa_{1-x}As$ layers were doped with Si and Sn from group-IV and S, Se, and Te from group-VI donor atoms. In addition, studies were carried out with the epitaxial layers removed entirely from the parent GaAs substrates, attached to substrates with larger lattice constants, and under applied uniaxial stresses. The present measurements demonstrate explicitly the influence of chemically different donor species on the nature of the shallow donor states in AlAs and $Al_xGa_{1-x}As$ ($x \geq 0.35$). In addition, the hydrogenic effective-mass states are found to be modified by the heteroepitaxial strain in these layers. Also, the results provide evidence that the character of the donor states for a given impurity species in $Al_xGa_{1-x}As$ crystals changes as a function of aluminum mole fraction.

The paper is divided into five sections. In Sec. II a brief description of the optically detected magnetic-resonance technique, table of sample parameters, descriptions of the ion-implantation and substrate-removal procedures, and additional experimental details are given. In Sec. III the theory of the donor ground state within the virtual-crystal approximation (VCA) in $Al_xGa_{1-x}As$ for group-IV and group-VI impurities substitutional on the III or V lattice sites, respectively, is reviewed. The results of the optically detected magnetic-resonance experiments are presented in Sec. IV. General features and trends are summarized. In Sec. V a discussion of the results and comparison with recent models proposed by several groups are made. A summary and overall conclusions of this work are provided in Sec. VI.

II. EXPERIMENTAL DETAILS

The ODMR experiments were performed on a comprehensive set of epitaxial layers with thicknesses from 1–7 μm of $Al_xGa_{1-x}As$ ($x \geq 0.35$) and AlAs doped with Si-, Sn-, S-, Se-, or Te-donor atoms on 350–500-μm-thick (001) semi-insulating GaAs substrates. A variety of growth techniques were employed for these studies, including molecular-beam epitaxy (MBE), liquid-phase epitaxy (LPE), and organometallic vapor-phase epitaxy (OMVPE). The AlAs mole fraction (x), layer thickness, particular dopant, and nominal donor concentration of these samples are summarized in Table I. In addition, a thick undoped $Al_xGa_{1-x}As$ buffer layer was grown between the GaAs substrate and n-doped $Al_xGa_{1-x}As$ layer in most of the samples to prevent the formation of a two-dimensional electron-gas sheet at the substrate-epilayer interface. The samples cleaved from these wafers were typically 2.5×7.0 mm^2. The aluminum mole fraction for most of the samples was determined by double-crystal x-ray measurements.

Two pieces from the same undoped LPE-grown wafer with $x = 0.6$ were ion implanted with Si and S atoms. Similarly, an undoped sample grown by OMVPE with AlAs mole fraction $x = 0.4$ was studied before and after S-ion implantation. A multiple-energy implantation procedure followed by a 10 s, 850 °C close-contact anneal in an inert atmosphere was employed to produce spatially uniform dopant profiles extending approximately 4000 Å from the $Al_xGa_{1-x}As$ surfaces.

ODMR measurements were obtained also on some of the $Al_xGa_{1-x}As$ and AlAs layers after removal from the parent GaAs substrates. The GaAs substrates were removed by lapping with 5 μm grain-size aluminum-oxide powder, followed by a fast nonselective GaAs/AlAs etch, and finally, by a slow GaAs selective etch. In addition, a freestanding layer of Si-doped AlAs was studied after mounting the epilayer on a silica rod with a thin glue layer composed of rubber cement.

The magnetic resonance was detected synchronously as a change in the total intensity of photoluminescence (PL) which was coherent with the on-off switching of 50 mW of microwave power at frequencies from 77–500 Hz in a K-band (24 GHz) spectrometer. PL was continuously excited with above-band-gap radiation provided by a Kr^+ laser at 476 nm or an Ar^+ laser at 458 nm with power

TABLE I. Summary of the pertinent parameters of the *n*-doped $Al_xGa_{1-x}As/GaAs$ heterostructures investigated in this work.

Sample designation	Growth technique	AlAs mole fraction (x)	Layer thickness (μm)	Dopant	Concentration (cm^{-3})
1	MBE	0.41	1.5	Si	5×10^{16}
2	MBE	0.50	1.5	Si	5×10^{16}
3	LPE	0.59	1.0	Si	1×10^{17}
4	MBE	0.72	1.5	Si	1×10^{18}
5	OMVPE	1.0	5.5	Si	1×10^{18}
6	OMVPE	0.45	4.0	Sn	5×10^{16}
7	OMVPE	0.60	3.0	Sn	1×10^{17}
8	OMVPE	1.0	7.0	Sn	3×10^{17}
9[a]	OMVPE	0.40	5.0	S	5×10^{16}
10[a]	LPE	0.59	1.0	S	3×10^{17}
11	OMVPE	0.60	1.2	Se	5×10^{17}
12	MBE	0.40	2.0	Te	2×10^{17}
13	MBE	0.60	2.0	Te	2×10^{17}

[a]Implanted and annealed.

densities between 0.1 and 1 W/cm^2. Deep photoluminescence from 1.0–1.8 μm was detected by a Northcoast liquid-nitrogen-cooled Ge photodiode. Band-edge PL in the visible spectral region was detected by a room-temperature Si photodiode. The samples were studied under pumped-helium conditions ($T\simeq1.6$ K) in a commercial optical cryostat.

The data presented in this work were obtained with a 9-in. pole-face electromagnet with a maximum field of 1.1 T. The measurements were obtained in the Voight geometry in which the applied magnetic field (**B**) is perpendicular to the wave vector of the excitation radiation. Two sample geometries were employed so that the magnetic field could be rotated in the $(1\bar{1}0)$ and (001) crystal planes. Details of how the excitation light was coupled to the samples in the two orientations are given elsewhere.[14] Calibration of the g values for the ODMR system was carried out by EPR measurements of α, α'-diphenyl-β-picrylhydrazyl.

ODMR experiments were also performed on some of the $Al_xGa_{1-x}As/GaAs$ heterostructures with uniaxial stress applied in the plane of the epilayers along the $[1\bar{1}0]$ and [100] directions. The uniaxial stress was applied by hanging weights at one end of a rigid lever arm located above the cryostat. The other end of the lever arm was positioned above a $\frac{1}{8}$-in.-o.d. stainless-steel tube located along the central axis of the cryostat. The sample was placed between two $\frac{1}{8}$-in.-o.d. polystyrene cylinders. One cylinder was fixed to the bottom of the microwave cavity and the other mounted at the end of the stainless-steel tube. The cross section of the samples for these experiments was 0.75×0.50 mm^2 so that pressures up to 200 MPa (2 kbar) could be easily achieved. The length was ~2 mm to avoid bowing and stress inhomogeneity.

III. THEORETICAL BACKGROUND

The starting point for the theory of band states and shallow (band-related) impurities in $Al_xGa_{1-x}As$ is the VCA.[18] For the mixed sublattice, a potential is assumed which is the average cation (Al,Ga) potential appropriate to the alloy composition. Also, the atoms of both sublattices are assumed to occupy true lattice sites. Hence, the Bloch theorem applies, and band states are expected. Although the VCA has been generally successful in describing results in $Al_xGa_{1-x}As$, it will be necessary to go beyond this approximation to explain the ODMR results.

The conduction-band edges, the hydrogeniclike shallow donor levels associated with these minima, and the DX level in $Al_xGa_{1-x}As$ as a function of aluminum mole fraction within the VCA are shown in Fig. 1. The conduction-band minimum is located at the Γ point for $Al_xGa_{1-x}As$ crystals with Al mole fraction less than ap-

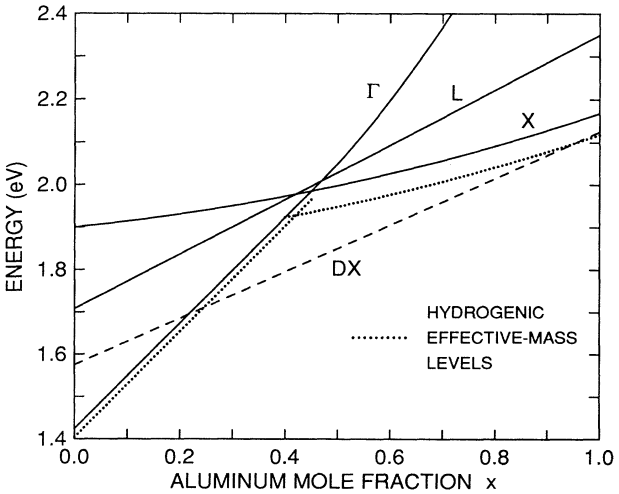

FIG. 1. Conduction-band minima (relative to the valence-band edge) and donor states in $Al_xGa_{1-x}As$ as a function of Al mole fraction (x). The effective-mass donor levels associated with the Γ and X minima are shown as dotted lines and the deep state (DX) of the donor is shown as a dashed line.

proximately 0.37. Far-infrared absorption measurements of the ground ($1s$) to first-excited-state ($2p$) transition associated with the Γ-derived shallow bound state have been observed in Si-doped $Al_xGa_{1-x}As$ with low-x values.[19,20] For x values ≥ 0.37, the position of the conduction-band minima abruptly changes from the Γ point to the X points. In addition, the conduction-band edge derived from the L points located along the $\langle 111 \rangle$ axes is nearly degenerate with those derived from the Γ and X points near $x=0.4$. Finally, the energy separations between the L and X conduction-band edges and the Γ and X conduction-band edges increase rapidly as x increases from 0.4 to 1.

The theory of the donor ground state in $Al_xGa_{1-x}As$ with high- (i.e., $x \geq 0.35$) AlAs mole fraction for group-IV and group-VI impurities substitutional on the III or V lattice sites, respectively, can be described within the VCA following work by Morgan.[21] The conduction-band constant-energy surfaces are ellipsoidal in momentum space about the X-point minima with long axes along the $\langle 001 \rangle$ cube-edge directions (see Fig. 2). In the hydrogenic effective-mass approximation, the wave function of the donor ground state is derived from (1) Bloch functions for the X_x, X_y, and X_z valleys and (2) $1s$-like envelope functions that satisfy the effective-mass equation. From symmetry arguments, the location of the donor atom in the lattice governs the degree to which the three hydrogenic effective-mass states will interact. For group-IV donors on the group-III site, the central cell potential does not mix the three hydrogenic effective-mass states. Thus, the ground state of an electron bound to a group-IV donor is an orbital (valley) triplet (T_2 in the T_d group). Therefore, neglecting spin-orbit interactions and random strains, the ground state associated with a group-IV donor is threefold degenerate. However, the degeneracy can be lifted by a large uniaxial stress applied in a direction that removes the equivalence of the three X-point conduction-band minima. This has been demonstrated from EPR studies of Sn donors in GaP under applied uniaxial stress.[22]

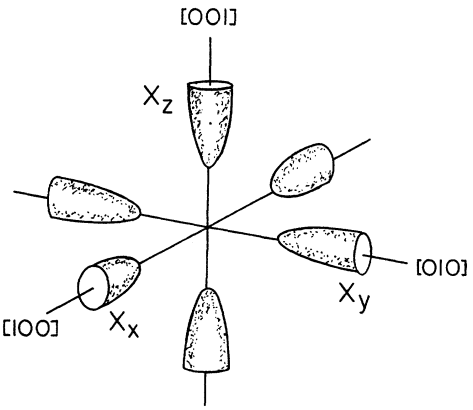

FIG. 2. Schematic diagram of the conduction-band constant-energy ellipsoids about the X-point minima in momentum space for AlAs.

The nature of the predicted donor ground state for group-VI impurities in $Al_xGa_{1-x}As$ with $x \geq 0.35$ is quite different. The central cell potential for group-VI donors on the group-V site strongly admixes the three hydrogenic effective-mass states. As a result, an orbital singlet (A_1) ground state is formed from the symmetric combination of the hydrogenic effective-mass states with a binding energy greater than the energy level determined from effective-mass theory ($\sim 40-50$ meV). A twofold-degenerate excited state (E) remains near the effective-mass energy level. The different in energy between the singlet ground state and the doublet excited state for a given donor species is commonly referred to as the valley-orbit splitting (E_{12}) or chemical shift. For example, chemical shifts have been observed in the ionization energies for various group-VI donor impurities in GaP.[23] However, unusually large chemical shifts of the ground-state donor levels have been reported for group-IV impurities in a III-V semiconductor. For example, an anomalous deepening of the ground-state donor level was found for Ge in GaP.[24,25]

One of the most important parameters obtained from the ODMR experiments is the g factor. It is instructive to examine the single-valley g values associated with the X-point conduction-band minima, $g_\parallel$ and $g_\perp$ predicted using the theory of Roth[26] for donor electrons in $Al_xGa_{1-x}As$ ($x \geq 0.35$) as a function of Al mole fraction (x).[27] These g factors differ from the free-electron g value (2.0023), in the virtual-crystal approximation, due to the spin-orbit coupling between the X_3 conduction band and the uppermost spin-orbit split valence band:

$$g_\parallel(x)=2.0023-[\Delta_2(x)/E_2(x)][m_e/m_\perp(x)-1] , \quad (1)$$

$$g_\perp(x)=2.0023-[\Delta_2(x)/E_2(x)][m_e/m_\parallel(x)-1] , \quad (2)$$

where $m_\perp$ and $m_\parallel$ are the transverse and longitudinal conduction-band effective masses, Δ_2 is the spin-orbit splitting of the uppermost valence band, and E_2 is the interband, direct transition at the X point. The E_2 and $E_2+\Delta_2$ critical-point energies have been reported recently for the entire range of aluminum mole fraction in $Al_xGa_{1-x}As$ alloys.[28] The longitudinal ($m_\parallel$) and transverse ($m_\perp$) effective masses associated with the X-point conduction energy ellipsoids are not well known. However, values for these masses in the binary compounds GaAs and AlAs determined from calculations and experiments are available.[29] For example, using Eqs. (1) and (2) with $m_\perp=0.19m_e$ and $m_\parallel=1.1m_e$ gives $g_\parallel=1.915$ and $g_\perp=2.004$ for electrons in AlAs.

IV. RESULTS AND ANALYSES

A. Photoluminescence

The magnetic-resonance results described below were obtained mainly on deep recombination processes in these samples. Some general trends were observed irrespective of the particular dopant or Al mole fraction. Representative PL spectra obtained from several $Al_{0.6}Ga_{0.4}As$ samples doped with each of the chemically different donor species investigated in this work are

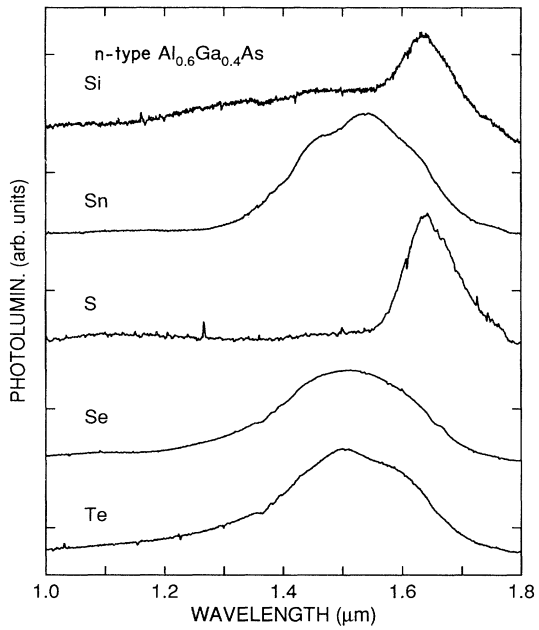

FIG. 3. Deep photoluminescence spectra obtained from several n-doped $Al_{0.6}Ga_{0.4}As$ epitaxial layers at 1.6 K with 50 mW of 476-nm excitation.

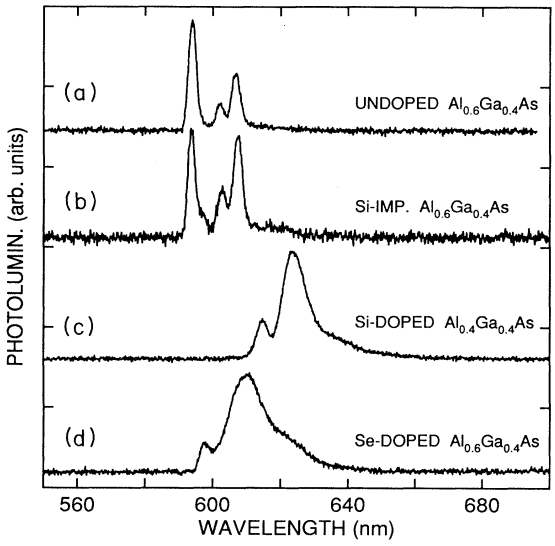

FIG. 4. Near-band-edge photoluminescence spectra obtained from several undoped and n-doped $Al_xGa_{1-x}As$ samples at $T=1.6$ K.

shown in Fig. 3. Most of the as-grown and implanted $Al_xGa_{1-x}As$ and AlAs layers grown by OMVPE exhibited a single, broad deep PL band with peak spectral response at 1.5 μm (0.8 eV). Little or no deep luminescence was found in the nominally undoped $Al_{0.6}Ga_{0.4}As$ layer grown by LPE. However, strong PL bands were found at $\sim$1.64 μm (0.74 ev) *after* Si- or S-ion-implantation procedures. The PL bands observed from the three Si-doped $Al_xGa_{1-x}As$ layers with $x=0.41$, 0.50, and 0.72 grown by MBE exhibited typically the broadest near-infrared spectral response among all the samples. Emission was found in these three particular samples extending from 1.0–1.7 μm.

In addition to the deep photoluminescence, strong band-edge emission was observed in most of the n-doped $Al_xGa_{1-x}As$ layers with Al mole fraction less than 0.7. However, except for a couple of cases, the magnetic-resonance signals detected as changes in the band-edge emission intensities from these samples were quite weak. Representative near-band-edge PL spectra obtained from several undoped and n-doped $Al_xGa_{1-x}As$ layers are shown in Fig. 4. The Al mole compositions determined from the highest energy PL bands in these samples and extrapolations of published PL data[30] for x in the indirect region were usually within 10% of the values found from the double-crystal x-ray measurements. The sharpest bands were found for the undoped or ion-implanted (Si or S) $Al_{0.6}Ga_{0.4}As$ layers grown by LPE. The excitonic emission for these samples was detected at 594 nm (2.088 eV) with a width of 12 meV. The bands at 599 nm (2.070 eV) and 607 nm (2.043 eV) were observed to increase relative to the highest energy peak after Si or S implantation. The dominant near-band-edge PL bands observed from the n-doped $Al_xGa_{1-x}As$ samples ($x \leq 0.7$) grown by MBE or OMVPE were typically much broader than the weaker excitonic emission peaks at higher energy [see Figs. 4(c) and 4(d)].

B. Optically detected magnetic resonance

The results of the ODMR studies are divided into three subsections. First, results are shown for the Si-doped AlAs and $Al_xGa_{1-x}As$ layers. Next, ODMR spectra from the Sn-doped AlAs and $Al_xGa_{1-x}As$ layers are presented. Finally, ODMR results obtained on deep luminescence from the $Al_xGa_{1-x}As$ layers doped with group-VI impurity atoms are given.

1. Si donors in AlAs and $Al_xGa_{1-x}As$

Results were obtained for the magnetic field (**B**) applied in the (1$\bar{1}$0) and (001) planes of a Si-doped AlAs/GaAs heterostructure (see Fig. 5). In the former geometry (top half of Fig. 5), a single line is observed that shifts from $g=1.945\pm0.001$ for **B**$\|$[110] to $g=1.978\pm0.001$ for **B**$\|$[001], the growth axis. In the latter geometry (bottom half of Fig. 5), two resonances with approximately equal amplitudes are found with $g=1.917\pm0.001$ and $g=1.976\pm0.001$ for **B**$\|$[100]. A single line is observed again with $g=1.947\pm0.001$ as the magnetic field is rotated to the [110] direction. No differences are observed in the linewidths or g values of the two well-resolved resonances with **B** along the third cube-edge direction (i.e., [010]). A compilation of the g values obtained from the angular-rotation studies performed on this sample is given in Fig. 6. An overall tetragonal symmetry of the resonance about the [001] axis is found.

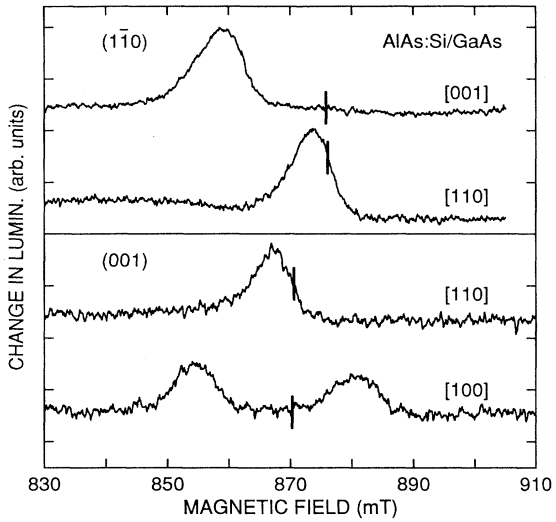

FIG. 5. ODMR spectra obtained for the Si-doped AlAs/GaAs heterostructure with **B** rotated in the (1$\bar{1}$0) and (001) planes. Vertical bars indicate $g=1.94$.

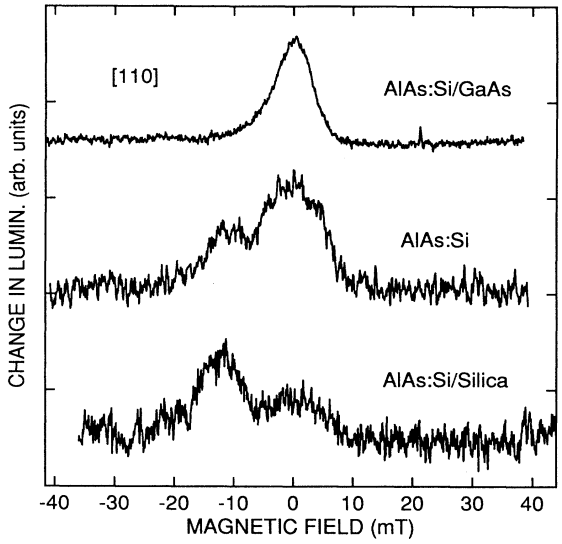

FIG. 7. ODMR spectra obtained for the Si-doped AlAs layers studied under different heteroepitaxial strain conditions. Top spectrum: biaxial compression. Middle spectrum: ~0 strain. Bottom spectrum: biaxial tension.

ODMR studies were performed also on the Si-doped AlAs sample after removal from the parent GaAs substrate as described in Sec. II. In addition, ODMR measurements were made after attaching the AlAs:Si freestanding layer to a silica substrate. Spectra for the three unique substrate conditions with **B**||[110] are shown in Fig. 7. Clear differences are observed in these spectra. In marked contrast to the result obtained with the AlAs layer on the GaAs substrate, two resonances are observed with the layer removed from the substrate or mounted on a substrate with a larger lattice constant at low temperatures. The g values (1.949±0.001) of the higher-lying magnetic field resonance are identical within error to that found for the single line from the AlAs/GaAs heterostructure. Also, the g values extracted from the lower-lying magnetic field resonances are nearly equal: 1.975±0.001 for the freestanding AlAs:Si sample versus 1.978±0.001 for the AlAs:Si/silica sample. Finally, the amplitude of the higher-lying field resonance was approximately twice that of the lower-lying resonance in the freestanding layer. The opposite behavior was found in the AlAs:Si/silica sample.

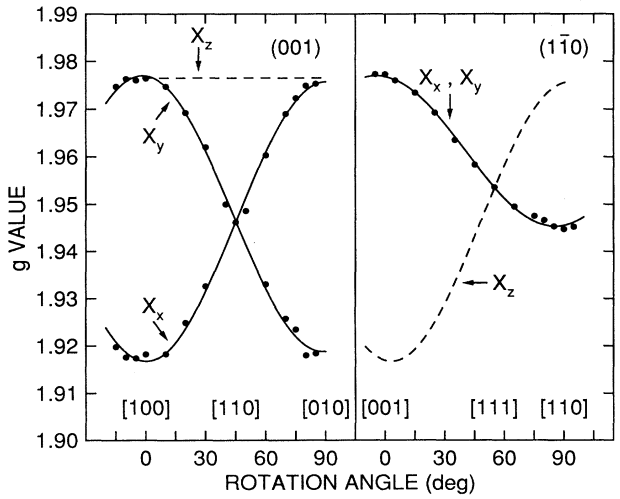

FIG. 6. Donor g values for two crystallographic planes for the Si-doped AlAs/GaAs heterostructure. The solid lines are fits to the data as described in the text. The dashed lines depict the additional rotation patterns that would be found if effective-mass states derived from the X_z valley were also populated.

ODMR spectra were obtained on the Si-doped $Al_xGa_{1-x}As$/GaAs samples for several values of aluminum mole fraction (x) with **B** parallel to the [100] direction (see Fig. 8). The most significant trend of these spectra is the decrease in splitting between the two resonances with decreasing aluminum mole fraction. It is found that only one resonance peak can be resolved in this geometry for the sample with $x=0.41$.

A compilation of the g values as a function of AlAs mole fraction from the ODMR experiments on the Si-doped AlAs/GaAs and $Al_xGa_{1-x}As$/GaAs heterostructures is shown in Fig. 9. Several features are important. First, the g-value anisotropy of the single line observed with the field in the (1$\bar{1}$0) plane decreases rapidly with decreasing Al mole fraction. Second, the g values obtained with the magnetic field along the [100] direction shift monotonically towards $g=1.94$ as x approaches 0.4. Third, the g values obtained with the magnetic field along the [110] direction are found to be approximately constant ($g\sim1.94$). Finally, the ODMR features described above were observed *only* for samples with aluminum mole fraction greater than ~0.35.

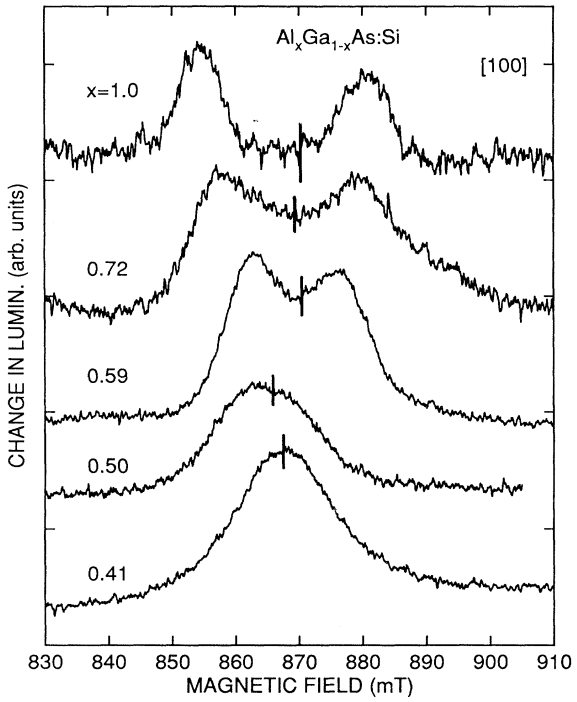

FIG. 8. ODMR spectra obtained for several Si-doped $Al_xGa_{1-x}As/GaAs$ samples with $\mathbf{B}\|[100]$. Vertical bars indicate $g=1.94$.

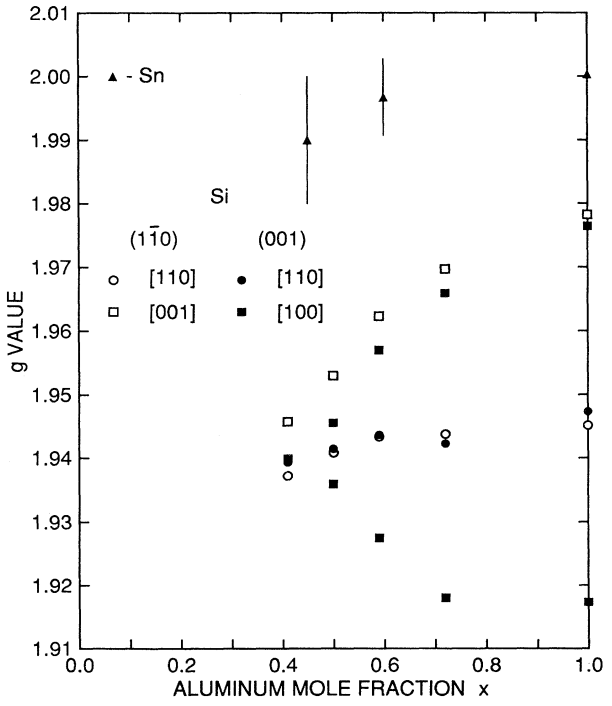

FIG. 9. Compilation of the ODMR g values as a function of AlAs mole fraction (x) with $\mathbf{B}$ rotated in the (1$\bar{1}$0) and (001) planes. Open and closed squares and circles: Si-doped samples with the error in g values $=\pm 0.001$. Closed triangles: Sn-doped samples. The g values are isotropic for the resonances observed from the Sn-doped $Al_xGa_{1-x}As$ samples.

A general trend is observed also in the linewidths of the ODMR spectra obtained for the Si-doped $Al_xGa_{1-x}As/GaAs$ heterostructures. The full widths at half-maximum amplitude of the resonances observed with the applied magnetic field oriented parallel and perpendicular to the [001] axis are plotted as a function of aluminum mole fraction in Fig. 10. The linewidths for both geometries increase with decreasing aluminum mole composition. The largest change in linewidth is found for samples with x near the direct-indirect gap crossover region (i.e., $0.37 \leq x \leq 0.42$).

Additional experiments to probe the source or sources of the ODMR linewidths in the Si-doped $Al_xGa_{1-x}As$ samples with x near 0.4 were also carried out. The linewidth was insensitive to changes in either the excitation power (varied from 0.5 to 200 mW) or microwave chopping frequency (varied from 35 to 5000 Hz). However, the linewidth did change significantly when studied in a Q-band (35 GHz) spectrometer (see Fig. 11). The linewidth of the donor resonance in Si-doped $Al_{0.5}Ga_{0.5}As$ with $\mathbf{B}\|[001]$ increased from 11 mT at 24 GHz to 16 mT at 35 GHz. Note this increase scales with the ratio of the two microwave energies. Previous measurements[13] at 9 GHz reveal linewidths smaller than the 24-GHz results. This behavior may indicate a distribution in g values.

ODMR experiments were performed also with externally applied uniaxial stresses for samples with intermediate Al mole fractions. Representative spectra for a Si-doped $Al_{0.4}Ga_{0.6}As/GaAs$ heterostructure with uniaxial stress applied in the [1$\bar{1}$0] and [100] directions are shown in Fig. 12. A compilation of the g values as a function of the magnitude of the stress for the two geometries is given in Fig. 13. There is no shift of the g values and lit-

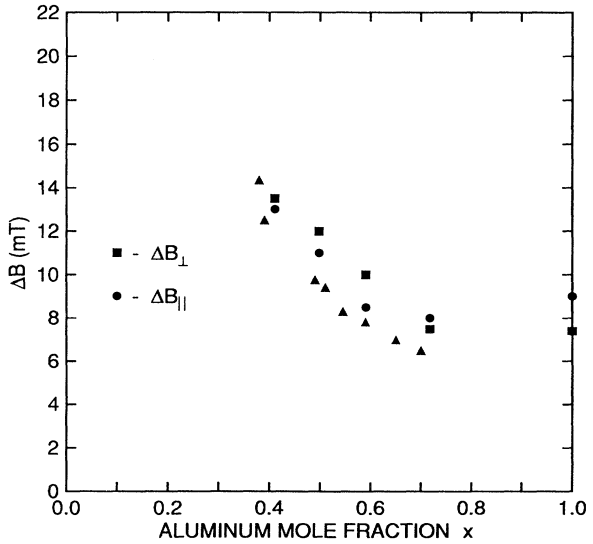

FIG. 10. Plot of the ODMR linewidths with $\mathbf{B}$ oriented parallel and perpendicular to the [001] growth direction for the Si-doped $Al_xGa_{1-x}As$ layers on the GaAs substrates. Triangles: X-band data (Ref. 12).

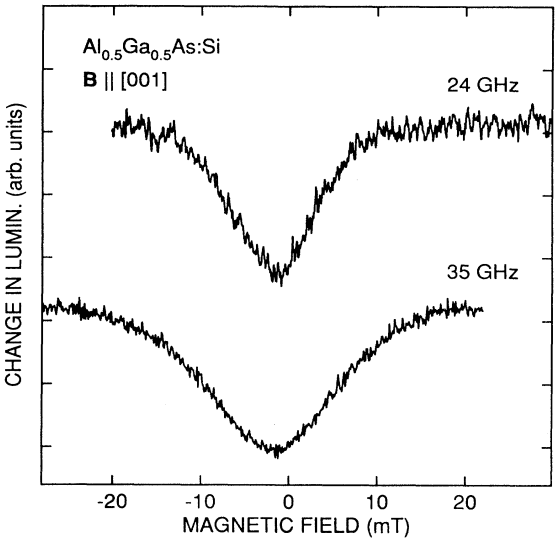

FIG. 11. Comparison of the ODMR spectra obtained for the Si-doped $Al_{0.5}Ga_{0.5}As/GaAs$ sample at 24 and 35 GHz. The spectra are displayed about $g=1.95$ ($\mathbf{B}\equiv 0$) to account for the different microwave frequencies.

tle change in the linewidth of the resonance up to the maximum stress applied in the [1$\bar{1}$0] direction. However, an immediate change in the character of the resonance is observed with stress along the [100] cube-edge direction in the plane of the epilayer. The g value of the resonance

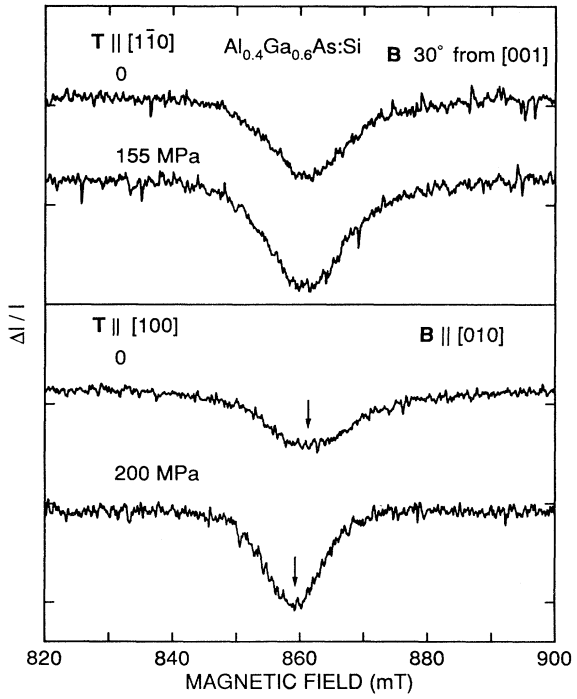

FIG. 12. ODMR spectra obtained for the Si-doped $Al_{0.4}Ga_{0.6}As/GaAs$ heterostructure with uniaxial stress ($\mathbf{T}$) applied in the [1$\bar{1}$0] (top half) and [100] (bottom half) directions.

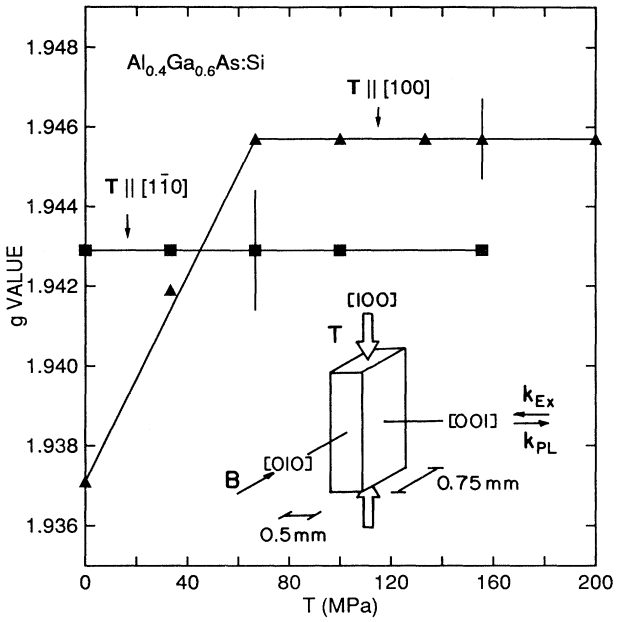

FIG. 13. ODMR g-values for Si donors in $Al_{0.4}Ga_{0.6}As$ with uniaxial stress applied in the [100] (triangles) and [1$\bar{1}$0] (squares) directions. $\mathbf{B}\|[010]$ for $\mathbf{T}\|[100]$ and 30° from [001] for $\mathbf{T}\|[1\bar{1}0]$. Solid lines are guides to the eye. Inset: sample geometry for $\mathbf{T}\|[100]$.

with $\mathbf{B}\|[010]$ shifts from 1.937 ± 0.001 for $|\mathbf{T}|=0$ to 1.946 ± 0.001 for $|\mathbf{T}|\simeq 60$ MPa. The g value does not shift further for larger values of stress. Note that this limiting g value is equal within error to that obtained with the field oriented along [001] in the absence of externally applied stresses (see Fig. 9). In addition, the linewidth of the resonance narrows with increasing stress from ~ 15.8 mT to a limiting value of ~ 10 mT.

2. *Sn donors in AlAs and $Al_xGa_{1-x}As$*

Magnetic-resonance spectra were obtained on luminescence from the Sn-doped AlAs/GaAs heterostructure for several orientations of $\mathbf{B}$ in the (1$\bar{1}$0) plane (see Fig. 14). The deep PL band in this sample was found at 1.1 eV, unique compared to the emission peaks at 0.8 eV observed from the most of the n-doped $Al_xGa_{1-x}As$ samples investigated in this work. Two distinct resonances are observed. First, a single, luminescence-decreasing feature with $g=2.091$ was found with $\mathbf{B}\|[110]$. The g value of the resonance is isotropic, but the intensity of this line diminishes as $\mathbf{B}$ is rotated from [110] to [001]. Second, a broad, luminescence-increasing resonance was observed with the field oriented away from [110]. The intensity of this feature increases as $\mathbf{B}$ approaches [001] in the (1$\bar{1}$0) plane. The g value of the resonances is 2.00 ± 0.02 and the FWHM ~ 150 mT with $\mathbf{B}\|[001]$. Also, the g value is isotropic within experimental error as determined from the spectra obtained with field orientations where the positive broad line is the dominant feature.

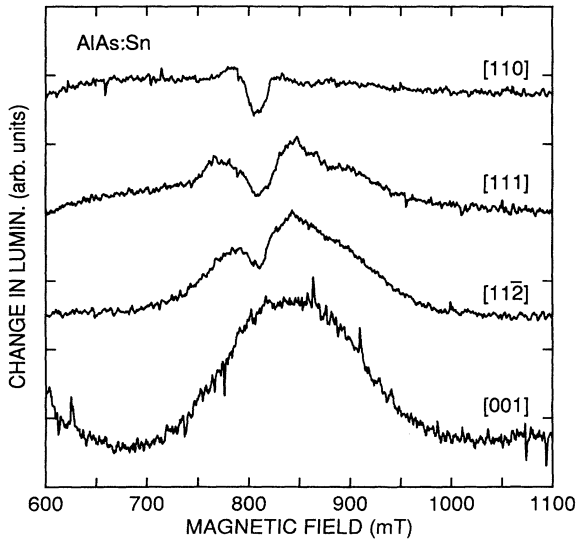

FIG. 14. ODMR spectra obtained for the Sn-doped AlAs/GaAs sample with the magnetic field rotated in the (1$\bar{1}$0) plane.

Representative ODMR spectra for a Sn-doped $Al_{0.6}Ga_{0.4}As/GaAs$ sample with the field rotated in the (1$\bar{1}$0) plane are shown in Fig. 15. Two unique resonances are observed again. First, the dominant feature is an isotropic, luminescence-increasing resonance with $g=1.997\pm0.006$ and FWHM $\simeq 50$ mT. The intensity of this line is fairly insensitive to the orientation of the applied field in the (1$\bar{1}$0) plane. Second, an isotropic, four-line spectrum was also observed. The third peak of the four-line spectrum is probably masked by the strong positive resonance with $g=1.997$ described above. A similar spectrum has been reported recently from ODMR studies[31] of undoped $Al_xGa_{1-x}As$ ($0.17\leq x\leq 0.65$) grown by metal-organic vapor-phase deposition. The g values of the dominant resonances observed in the three Sn-doped $Al_xGa_{1-x}As$ layers ($0.45\leq x\leq 1$) investigated in this work are plotted in Fig. 9 (solid triangles). The g values are equal (~ 2.00) within experimental error.

3. *Group-VI donors (S, Se, Te) in $Al_xGa_{1-x}As$*

The group-VI donors S, Se, and Te have also been studied. Representative ODMR spectra for a Se-doped $Al_{0.6}Ga_{0.4}As/GaAs$ sample are shown in Fig. 16. The general behavior of the resonances observed in this structure are found also in the $Al_xGa_{1-x}As$ layers ($x=0.4$, 0.6) doped with either S or Te. Results were obtained again with **B** applied in the (1$\bar{1}$0) and (001) planes of the sample. In the (1$\bar{1}$0) plane, a single line was observed that shifts from $g=1.953\pm0.001$ for **B**$\|$[110] to $g=1.961\pm0.001$ for **B**$\|$[001]. In the (001) plane, a single isotropic line was observed with $g=1.953\pm0.001$. The spectra shown in Figs. 17 and 18 demonstrate explicitly the different ODMR characteristics between the Si-doped and group-VI-doped $Al_xGa_{1-x}As/GaAs$ heterostructures with aluminum mole fraction equal to 0.6. In the (1$\bar{1}$0) plane, the g-value anisotropy is much larger for the Si-doped sample ($\Delta g=0.020$) than for the Se-, S-, and Te-doped $Al_{0.6}Ga_{0.4}As/GaAs$ samples ($\Delta g=0.008-0.010$). In addition, two resonances are resolved in the Si-doped sample while the lines in the S-, Se-, and Te-doped samples are unsplit with the magnetic field applied along the [100] cube-edge direction.

A compilation of the g values as a function of AlAs mole fraction from the ODMR experiments on the $Al_xGa_{1-x}As$ epitaxial layers doped with group-VI atoms

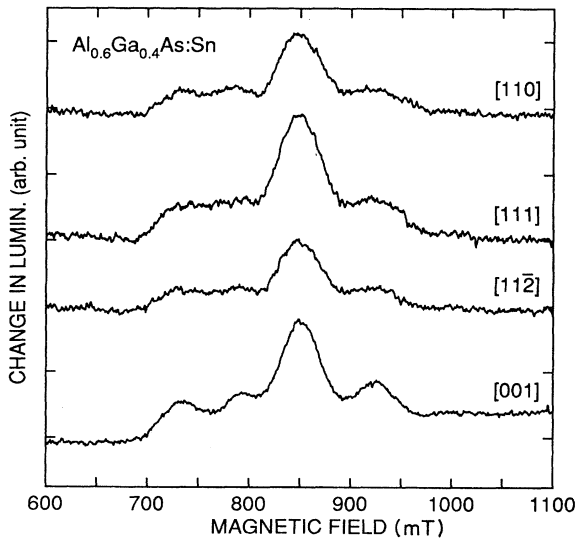

FIG. 15. ODMR spectra obtained for the Sn-doped $Al_{0.6}Ga_{0.4}As/GaAs$ heterostructure with **B** rotated in the (1$\bar{1}$0) plane.

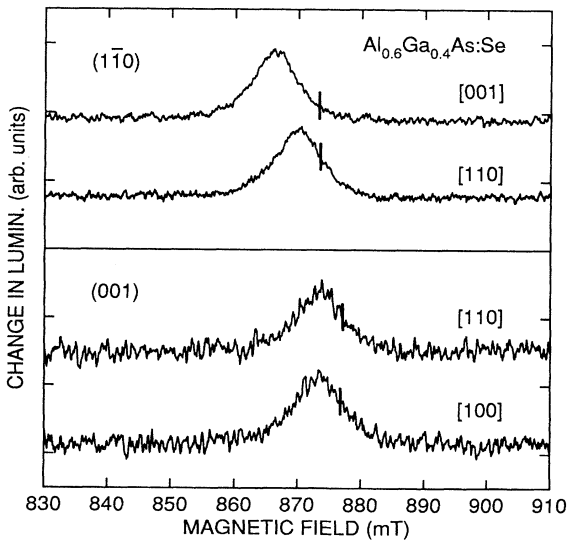

FIG. 16. ODMR spectra obtained for the Se-doped $Al_{0.6}Ga_{0.4}As/GaAs$ sample with **B** rotated in the (1$\bar{1}$0) and (001) planes. Vertical bars indicate $g=1.95$.

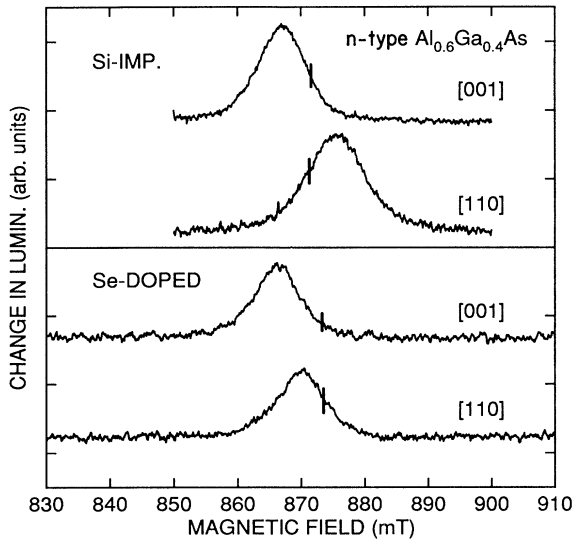

FIG. 17. Comparison of the ODMR spectra obtained for the Si- and Se-doped $Al_{0.6}Ga_{0.4}As/GaAs$ samples with **B** rotated in the $(1\bar{1}0)$ plane. Vertical bars indicate $g=1.95$.

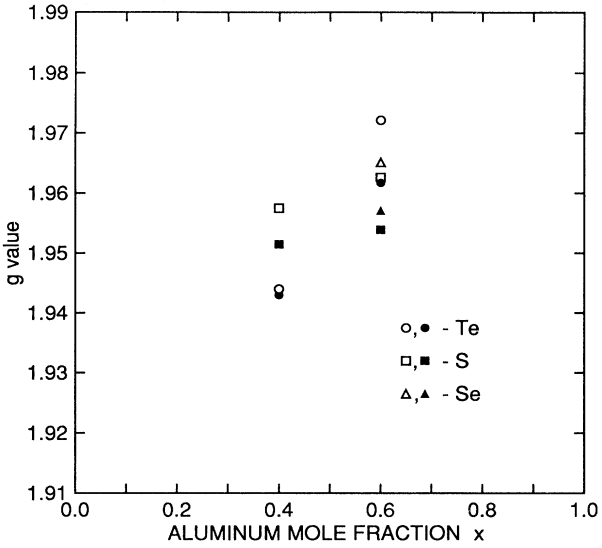

FIG. 19. Compilation of the ODMR g values for the group-VI-doped $Al_xGa_{1-x}As/GaAs$ heterostructures. Open symbols: $\mathbf{B}\|[001]$. Closed symbols: $\mathbf{B}\|[1\bar{1}0]$ (or $\|[100]$).

is shown in Fig. 19. As noted above, the g-value anisotropies in the $(1\bar{1}0)$ plane are similar ($\Delta g=0.008-0.010$) for the $Al_{0.6}Ga_{0.4}As$ samples doped with S, Se, or Te. However, slight differences were found in the absolute g values for these structures with the magnetic field along the [110] or [001] axes. In addition, the g-value anisotropy for the S-doped $Al_xGa_{1-x}As/GaAs$ heterostructure decreases from $\Delta g=0.008$ for $x=0.6$ to $\Delta g=0.006$ for $x=0.4$. However, the g value of the single line observed in the $(1\bar{1}0)$ plane of the Te-doped $Al_{0.4}Ga_{0.6}As/GaAs$ sample is nearly isotropic.

ODMR experiments were performed also on the Se-doped $Al_{0.6}Ga_{0.4}As$ sample after removal from the GaAs substrate. Representative ODMR spectra obtained from this study with the field in the $(1\bar{1}0)$ plane are shown in Fig. 20 along with the spectra described above for the epitaxial layer on the substrate. An *isotropic* line with $g=1.956\pm0.001$ was found for the freestanding sample in contrast to the anisotropic resonance observed from the Se-doped $Al_{0.6}Ga_{0.4}As/GaAs$ heterostructure.

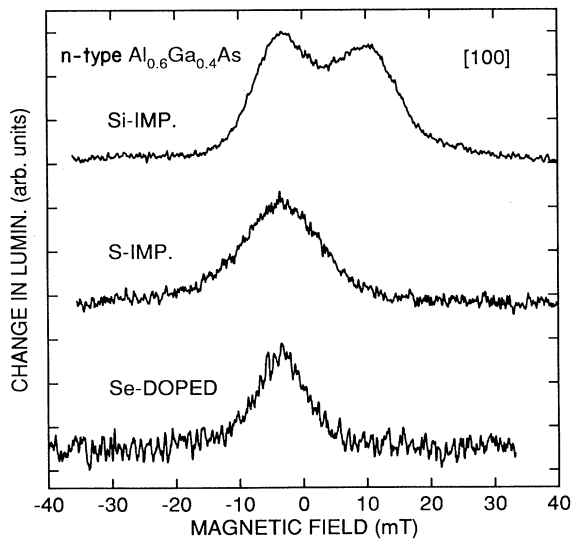

FIG. 18. Comparison of the ODMR spectra obtained for the Si-, Se-, and S-doped $Al_{0.6}Ga_{0.4}As/GaAs$ heterostructures with $\mathbf{B}\|[100]$. The spectra are displayed about $g=1.95$ ($\mathbf{B}\equiv0$) to account for the slightly different microwave frequencies.

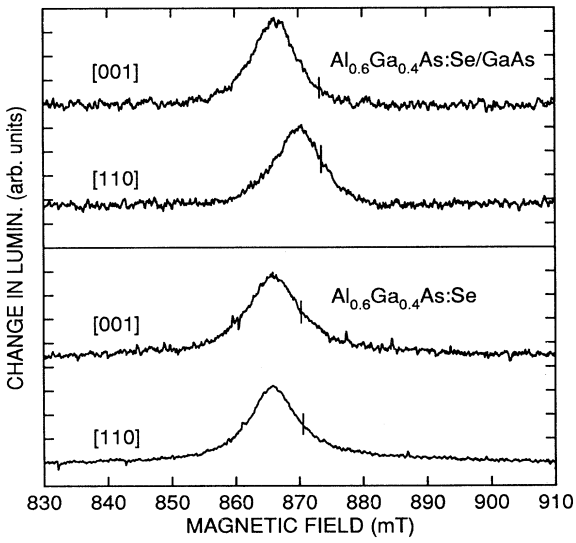

FIG. 20. Comparison of the ODMR spectra obtained for the Se-doped $Al_{0.6}Ga_{0.4}As$ sample studied with the epitaxial layer on the GaAs substrate (top half) and after removal from the substrate (lower half). Spectra are shown for two field directions in the $(1\bar{1}0)$ plane. Vertical bars indicate $g=1.95$.

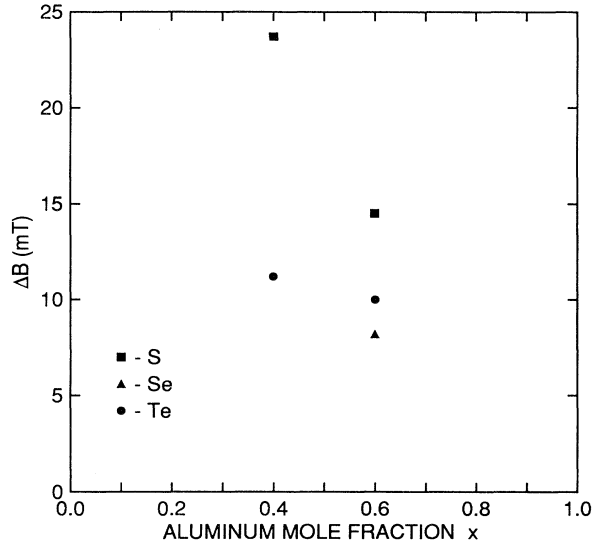

FIG. 21. Plot of the ODMR linewidths for the group-VI-doped $Al_xGa_{1-x}As/GaAs$ samples. The linewidths are fairly insensitive to the orientation of **B** in the $(1\bar{1}0)$ or (001) planes.

The linewidths of the ODMR spectra obtained for the group-VI-doped $Al_xGa_{1-x}As/GaAs$ samples are plotted as a function of aluminum mole fraction in Fig. 21. The individual linewidths are fairly insensitive to the orientation of the applied magnetic field in the $(1\bar{1}0)$ or (001) planes. The linewidths obtained for the S-implanted $Al_xGa_{1-x}As$ layers are larger compared to the linewidths found for the Se- and Te-doped samples. Also, the linewidth found for the S-implanted samples increases significantly with decreasing Al mole fraction.

V. DISCUSSION

A. AlAs:Si

The results for the Si-doped AlAs/GaAs heterostructure can be understood using an independent-valley model in the presence of strain. The mismatch of the AlAs and GaAs lattice constants at 1.6 K ($\Delta a/a = 1.4\times10^{-3}$) leads to a biaxial compression in the plane of the epilayer and an elongation along the [001] growth direction due to the Poisson effect. The heteroepitaxial stress raises the X_z valley relative to the X_x and X_y valleys. The strain-induced splitting is given by[32]

$$\Delta X = \Xi_u(e_\perp - e_\parallel) , \tag{3}$$

where Ξ_u is the shear deformation potential and $e_\perp$ and $e_\parallel$ are the perpendicular and in-plane lattice strains,[33] respectively, in the AlAs epitaxial layer. We estimate the valley splitting to be approximately 14 meV using the AlAs deformation potential $\Xi_u = 5.1\pm0.7$ eV deduced from recent piezospectroscopic studies of type-I and type-II GaAs/AlAs superlattices.[34] Thus, the X_z valley at 1.6 K is not populated and, hence, does not participate in the recombination. Two well-separated resonances of about equal intensities are observed with the magnetic field along the [100] direction (see the bottom half of Fig. 5) because the field is simultaneously oriented parallel to the long axis (g value denoted by $g_\parallel$) of the X_x valley and parallel to the short axis (g value denoted by $g_\perp$) of the X_y valley.[14] A single anisotropic resonance feature is observed as the field is rotated in the $(1\bar{1}0)$ plane (see the top half of Fig. 5), since this plane mirrors the X_x and X_y valleys.

These results indicate that (i) the X_x and X_y valleys are decoupled since the two resonances are so clearly resolved and (ii) states derived from the X_z valley do not participate in the recombination since only one resonance is observed for $\mathbf{B}\|[001]$. Fits have been made to the data obtained from the angular-rotation studies with the usual expression for the g values in the case of axial symmetry

$$g = (g_\parallel'^2\cos^2\theta + g_\perp'\sin^2\theta)^{1/2} , \tag{4}$$

where θ refers to the angle between the applied magnetic field and the [100] ([001]) axis with the field rotated in the (001) [$(1\bar{1}0)$] plane and $g_\parallel'$ and $g_\perp'$ are the g values associated with the magnetic field oriented parallel and perpendicular to the [100] ([001]) direction, respectively. As shown by the solid lines in Fig. 6, the fits are quite reasonable. The fits to the data obtained with the field rotated in the (001) plane (see the left half of Fig. 6) yield the single-valley g values associated with the X-point conduction-band minima in AlAs: $g_\perp = 1.976\pm0.001$ and $g_\parallel = 1.917\pm0.001$ with respect to the long axis of an ellipsoid. The dashed lines in Fig. 6 depict the rotation patterns that would be expected in the (001) and $(1\bar{1}0)$ planes if the X_z valley was also populated. Thus, the Si-donor ground state in AlAs can be described as a doublet with tetragonal symmetry about the [001] direction. In addition, the symmetry behavior of the resonance feature confirms the states' association with the X-point conduction-band minima and not with the Γ or L points.

The independent-valley picture employed to describe the nature of the Si-donor ground state in AlAs is consistent with Morgan's prediction of a weak valley-orbit interaction for a group-IV donor on a group-III site in a III-V semiconductor. However, due to the multiplicity of valleys associated with the X-point conduction-band minima and the finite spin ($\frac{1}{2}$) of the donor electron, a spin-valley coupling must also be considered since this interaction ($\lambda\mathbf{L}\cdot\mathbf{S}$) can mix the X_x, X_y, and X_z valleys. As noted recently by Kaufmann *et al.*,[15] it was suggested that λ scales with the difference between the atomic spin-orbit coupling constants of the impurity and that of the host atom it replaces. The ODMR results on the Si-doped AlAs layers reflect the fact that the difference between the atomic spin-orbit constants of Al and Si is quite small.

The ODMR results obtained for the Si-doped AlAs sample can be compared with the results of detailed EPR studies of Si and Sn donors in GaP due to the similarity in the orbital degeneracy of the ground states.[22,35] It was necessary to apply large uniaxial stresses in appropriate directions in order to observe EPR signals in the Si- and Sn-doped bulk GaP samples. The uniaxial stress

effectively decouples the spin-orbit mixed valleys. It is possible to correlate the increase of λ between Si donors in GaP (2.7 cm^{-1}) and Sn donors in GaP (11.3 cm^{-1}) with the larger difference in atomic mass numbers between Sn and Ga as compared to Si and Ga. As previously mentioned, the small value of λ deduced for Si donors in AlAs probably arises from the similarity of the atomic masses between Si (mass number, 28) and Al (mass number, 27). These ideas will be invoked again to describe the nature of the Sn donor state in AlAs and for Si donors in $Al_xGa_{1-x}As$ with $x<1$.

It has been suggested that random strains (ϵ) must also be present in the x-y plane of the AlAs layer in order to account for the (nearly) equal intensities of the two resonances observed with the field along the [100] or [010] cube-edge directions.[15] The distribution of these random strains is such that at certain donor sites the X_x valley is lowered in energy, while at other sites the ground state is associated with the X_y valley alone. The origin of the random in-plane strains in AlAs is not understood at present. However, the existence of in-plane strains to adequately describe the ODMR results obtained for the Si-doped AlAs sample may not be necessary if λ is small.

The ODMR results obtained on the Si-doped AlAs sample with the layer removed from the GaAs substrate or attached to a substrate with the larger lattice constant demonstrate further that the Si donors behave as a local probe of the strain fields in AlAs. The g values and relative amplitudes of the two resonances observed with the magnetic field along the [110] direction in the free standing AlAs:Si sample (see the middle trace in Fig. 7) are consistent with the field oriented parallel to the short axes of the X_z valley (lower field resonance) and at 45° to *both* the X_x and X_y valleys (higher field resonance). Without strain, donor states derived from all three valleys are populated. These results on the freestanding Si-doped AlAs layer again provide evidence for negligible valley-orbit interactions and negligible spin-orbit coupling among the X_x, X_y, and X_z valleys.

For the case of the AlAs:Si layer attached to the silica substrate, the larger lattice constant at 1.6 K of the silica relative to the AlAs layer leads to a biaxial tension in the AlAs epilayer.[36] As a result, the X_z valley is lowered relative to the X_x and X_y valleys. The unequal amplitudes of the resonances observed for this structure with **B** along [110] (see the bottom trace in Fig. 7) reflect the higher population of the donor states associated with the X_z valley in the presence of compression in the z direction due to the biaxial tension in the x-y plane.

B. Group-VI donors in $Al_xGa_{1-x}As$

The behavior of the donor resonances observed for the group-VI-doped $Al_xGa_{1-x}As/GaAs$ samples can be understood in most cases by taking into account the heteroepitaxial strain and a *strong* valley-orbit interaction (discussed in Sec. III) that couples the X_x, X_y, and X_z valleys for a group-VI donor on the group-V site. The analysis described below is found to be most applicable for the S-, Se-, and Te-doped $Al_{0.6}Ga_{0.4}As/GaAs$ structures and for the S-doped $Al_{0.4}Ga_{0.6}As/GaAs$ sample. First, an isotropic g value is expected for a pure singlet (A_1) ground state. However, a small g-value anisotropy about the [001] axis is observed in the $(1\bar{1}0)$ plane (see the top half of Fig. 16) because of the slight mixing between the ground (A_1) and excited (E) states. This interaction is due to the tensile strain along the [001] axis. The ground state is no longer a pure singlet state but is an admixture of the singlet and excited doublet states. The observed g-value anisotropy of the resonance partially reflects the g-value anisotropy associated with the doublet state.

Similar admixing effects on the behavior of donor g values have been observed in EPR investigations of shallow donor in Si under applied unaxial stress by Wilson and Feher,[37] and we follow their analysis. The valley-orbit splitting energies (E_{12}) between the ground (A_1) and excited (E) states in the absence of stress for the S-, Se-, and Te-doped $Al_{0.6}Ga_{0.4}As/GaAs$ samples and the S-doped $Al_{0.4}Ga_{0.6}As/GaAs$ heterostructure can be deduced from the donor g-value anisotropies observed in the $(1\bar{1}0)$ plane. The expression for the g shift due to the mixing between the ground and excited states with the strain along the [001] growth direction is

$$g(\theta)-g_0=(g_{\parallel}-g_{\perp})[1-(3\sin^2\theta)/2] \times[1-(1+3x'/2)(1+x'/3+x'^2/4)^{-1/2}] , \quad (5)$$

where $g(\theta)$ is the donor g value in the presence of strain, g_0 is the donor g value in the absence of strain, θ is the angle between the [001] stress axis and the applied magnetic field, $g_{\parallel}$ and $g_{\perp}$ are single-valley g values associated with the X-point conduction-band minima, and x' is the ratio of the strain energy ($\sim$8.4 meV for $x=0.6$, $\sim$5.6 meV for $x=0.4$) to the valley-orbit splitting energy (E_{12}). The values employed for $g_{\parallel}$ and $g_{\perp}$ are taken from the ODMR results on the Si-doped AlAs/GaAs sample where the valleys are independent. Thus, the values of g_0 and E_{12} can be determined from the donor g values with the magnetic field parallel ($\theta=0°$) and perpendicular ($\theta=90°$) to the [001] axis.

Equation (5) predicts an isotropic g value for **B** rotated in the (001) plane (i.e., $\theta=90°$). In agreement with this analysis, isotropic g values are observed in the (001) plane of the group-VI-doped $Al_xGa_{1-x}As$ samples (see, e.g., the bottom half of Fig. 16). In addition, an isotropic resonance is predicted by Eq. (5) in the absence of stress (i.e., $x'=0$) as found for the freestanding Se-doped $Al_{0.6}Ga_{0.4}As$ (see the bottom half of Fig. 20).

A consistent picture emerges for most of the results obtained for the AlGaAs layers doped with group-VI impurities. The values of g_0 and E_{12} deduced from the above analysis are summarized in Table II. First, the g_0 value determined from the analysis ($g=1.955\pm0.001$) is in excellent agreement with the g value of the isotropic resonance ($g=1.956\pm0.001$) found for the Se-doped $Al_{0.6}Ga_{0.4}As$ layer removed from the GaAs substrate. Second, the valley-orbit splitting energies (i.e., chemical shifts) are 16.5–20 meV for the group-VI-doped $Al_xGa_{1-x}As$ samples. The valley-orbit splitting energies

TABLE II. Values of g_0 (the g value in the absence of strain) and E_{12} (the valley-orbit splitting energy or chemical shift) for the group-VI donors in $Al_xGa_{1-x}As$ determined from an analysis of the ODMR results. Also shown are the differences in ionization energies between Si donors and the same group-VI donors in GaP found from donor-acceptor pair luminescence spectra.

			E_{12} (meV)	
Impurity	x	g_0	$Al_xGa_{1-x}As$	GaP[a]
S	0.6	1.957±0.001	19.0±1	22.1
Se	0.6	1.955	20.0	20.5
Te	0.6	1.965	16.5	7.7
S	0.4	1.954	18.0	

[a]See Ref. 23.

are quite similar in the S-doped $Al_xGa_{1-x}As$ samples with $x=0.4$ and 0.6. The decrease of the donor g-value anisotropy between these two samples simply reflects the reduction of heteroepitaxial strain with decreasing Al mole fraction. However, this stress analysis breaks down for the Te-doped $Al_{0.4}Ga_{0.6}As$ sample since a much larger g-value anisotropy ($\Delta g=0.006$) should have been observed rather than the nearly isotropic line ($\Delta g=0.001$) found with **B** rotated in the $(1\bar{1}0)$ plane. This result implies that the central cell interactions are quite strong in this sample and lead to a highly localized (A_1) ground state.

These results for the chemical shifts of shallow donor levels in $Al_xGa_{1-x}As$ ($x\geq 0.35$) can be compared with earlier measurements[23] of the ionization energies determined from donor-acceptor pair luminescence spectra of the *same* group-IV and group-VI substitutional donors in GaP. The difference in ionization energies between Si donors on the Ga site and either S, Se, or Te donors on the P site was found to be 7–22 meV. It is interesting to note that Te also has the smallest chemical shift among these group-VI dopants in GaP as found in the $Al_{0.6}Ga_{0.4}As$ samples.

In the theory of donors in $Al_xGa_{1-x}As$ ($x\geq 0.35$) within the VCA,[18] both the doublet excited state (E) associated with the group-VI donors and the triplet group state (T_2) associated with group-IV donors lie very close to the effective-mass energy level. Thus, the finite valley-orbit splitting energies ($E_{12}\sim 16.5$–20 meV) found for S, Se, and Te donors necessarily imply a larger binding energy for these donors than for Si donors in $Al_xGa_{1-x}As$ with $x=0.6$. Recent Hall-effect measurements on similarly doped $Al_{0.6}Ga_{0.4}As$ samples yield binding energies for the X-derived shallow donor state that contrast with the ODMR results. In particular, the binding energy of the shallow hydrogenic level is reported to be larger for Si donors (~75 meV) (Ref. 38) than for Te donors (~25 meV) (Ref. 39) in $Al_{0.6}Ga_{0.4}As$. However, these binding energies may be in error by a factor of 2 due to compensation. One approach to resolve this conflict may be direct determination of the hydrogenic effective-mass ground-state energy for each species by luminescence spectroscopy. However, one would also need to know the binding energy of the acceptor involved in the donor-acceptor pair recombination to accurately determine the donor binding energy.

C. Si donors in $Al_xGa_{1-x}As$

The behavior of the donor g values and linewidths of the resonances observed from the Si-doped $Al_xGa_{1-x}As/GaAs$ samples with $x<1$ presents the biggest challenge in terms of a complete picture for the nature of the donor ground state in $Al_xGa_{1-x}As$ with intermediate-to-high Al mole fraction. The monotonic decrease in splitting between the two resonances observed for $\mathbf{B}\|[001]$ (see Fig. 8), the monotonic decrease in g-value anisotropy of the single line observed with **B** rotated in the $(1\bar{1}0)$ plane (see Fig. 9), and the increase in the linewidth of the donor resonances with decreasing Al mole fraction (see Fig. 10) indicate a breakdown of the independent-valley model that was employed to describe the symmetry of the donor ground state in the Si-doped AlAs/GaAs heterostructure. These results strongly suggest the presence of one or more interactions in these samples that lead to a coupling interaction among the individual valleys associated with the X-point conduction-band minima or perhaps a coupling of the X-derived valleys with valleys derived from the Γ and/or L bands.

A number of mechanisms must be considered that can potentially influence the nature of the Si-donor ground state in the $Al_xGa_{1-x}As$ samples with $x<1$. These include a finite spin-valley coupling interaction, L-X (Γ-X) interband mixing, and alloy disorder. These interactions will be discussed below in light of the ODMR results presented in Sec. IV B 1. Overall, the nature of the donor state in Si-doped $Al_xGa_{1-x}As$ for samples with x near 0.4 is not as well understood as the states associated with Si donors in AlAs and the group-VI donors in $Al_{0.6}Ga_{0.4}As$.

First, the single-valley g values ($g_\parallel=1.915$ and $g_\perp=2.004$) determined from Roth's equations described earlier in Sec. III are in fairly good agreement (especially the $g_\parallel$ value) with the g factors obtained from the present ODMR studies of the Si-doped AlAs sample: $g_\parallel=1.917\pm0.001$ and $g_\perp=1.976\pm0.001$. However, if the g values (see Fig. 9) determined from the two resonances obtained with $\mathbf{B}\|[100]$ in the Si-doped $Al_xGa_{1-x}As$ samples with $x<1$ are taken as single-valley g values associated with independent-X valleys, Roth's equations within the VCA can satisfactorily account for the increase of $g_\parallel$ with decreasing x but cannot account for the decrease of $g_\perp$ with decreasing Al mole fraction [for example, Eqs. (1) and (2) predict $g_\parallel=1.954$ and $g_\perp=2.013$, respectively, for $x=0.4$].

Recently, the dependence of the g values and the linewidths of the resonances on the aluminum mole fraction has been attributed to effective-mass donor states with mixed X, L, and Γ character.[15] In particular, the g values obtained with the field along [100] and [001] (see Fig. 9) have been fitted with contributions from both the L and X bands. The mixing coefficient between donor states derived from these bands is largest, as expected (see

Fig. 1), for x near 0.4. However, the nearly constant average donor g values (~ 1.945) observed for the entire set of Si-doped $Al_xGa_{1-x}As$ layers in this work (see Fig. 9) is *not* consistent with a strong L-X interaction, unless $(g_L)_{av} \approx (g_X)_{av}$. In particular, Roth's equations predict that $g_\parallel$ associated with the L-point conduction-band minima varies from ~ 1.487 for AlAs to ~ 1.026 for GaAs (determined from reported values for the E_1 and $E_1+\Delta_1$ critical-point energies and the L-point conduction-band effective masses[36]), where $\parallel$ refers to the $\langle 111 \rangle$ axes.

In order to test explicitly the L-X character of the donor wave function, ODMR experiments with externally applied uniaxial stresses were performed. In particular, uniaxial stress studies on the Si-doped $Al_xGa_{1-x}As$ sample with $x=0.4$ provide the best case to probe the strength of L-X interband mixing. Since the long axes of the L-point conduction-band constant-energy ellipsoids are located along the $\langle 111 \rangle$ axes, the equivalency of the four L-point valleys should be removed with stress applied in the $[1\bar{1}0]$ direction. The maximum stress applied along $[1\bar{1}0]$ in this study was approximately equal to the value of the heteroepitaxial stress in AlAs on GaAs. As seen in Figs. 12 and 13, there is no shift of the g value and little change in the linewidth for this type of strain. This results provides evidence against the contribution of donor states derived from the L-point conduction-band minima at $x=0.4$.

However, there is a noticeable change in the character of the resonance with uniaxial stress applied in the [100] direction. Hence the donor wave function is still X-like at $x=0.4$. The shift of the g value from 1.937 to 1.946 with finite stress along [100] is attributed to either a decoupling of the mixed X_x and X_y valleys such that, among the X_x, X_y, and X_z valleys, *only* states derived from the X_x valley contribute to the donor state or a valley depopulation effect. The significant change in linewidth and the saturation behavior of the g value and linewidth with $\mathbf{T} \geq 80$ MPa along [100] can be associated with one of the two strongly overlapping resonances observed at zero stress with $\mathbf{B} \| [010]$. Following this line of analysis, the limiting g value (1.946) obtained with $T \geq 80$ MPa can be assigned to $g_\perp$ for a single X valley at $x=0.4$. The same g value was found at zero stress and $\mathbf{B}$ along [001]. This interpretation implies that the single-X-valley g values (i.e., $g_\parallel$ and $g_\perp$) depend on the Al mole composition. However, this line of analysis leads to the conclusion that the asymmetry (i.e., ellipsoidal character) of the X valleys is much reduced for $Al_{0.4}Ga_{0.6}As$. This is highly unlikely since the mass anisotropy (i.e., $m_\parallel/m_\perp$) associated with the X-point conduction band is very similar for GaAs and AlAs.[36] Thus, it is difficult to describe the donor state at $x=0.4$ as a purely hydrogenic effective-mass state derived from the X-point conduction-band minima within the VCA.

In light of the reason for weak spin-valley interaction for Si donors in AlAs as discussed in Sec. V A, this interaction may become significant in the alloy layers because of the much larger difference in atomic mass numbers between Si and Ga as compared to Si and Al. Thus, the X_x and X_y valleys would be most strongly coupled at $x=0.4$ in this picture. The state derived from the X_z valley at $x=0.4$ is located approximately 6 meV above the X_x and X_y valleys due to the heteroepitaxial stress and probably does not contribute to the donor state. Contrary to an earlier analysis,[9] the results of the uniaxial stress experiments provide evidence against a purely spin-valley coupled state at $x=0.4$. In particular, the $g_\perp$ value observed for the Si-doped AlAs sample ($g_\perp = 1.976 \pm 0.001$) should be recovered with $\mathbf{T} \| [100]$ and $\mathbf{B} \| [010]$ at some finite stress (see Fig. 13). Instead, as noted above, the limiting g value is 1.946, equal to that obtained with $\mathbf{B} \| [001]$ in the absence of stress.

An additional mechanism that can alter the nature of the Si-donor ground state in $Al_xGa_{1-x}As$ is alloy disorder. For a random alloy, the maximum alloy disorder occurs for $x=0.5$ and diminishes in a linear fashion on either side of $x=0.5$. However, the ODMR spectra obtained for the Si-doped $Al_xGa_{1-x}As$ epitaxial layers that should have similar alloy disorder (i.e., the samples with $x=0.4$ and 0.6) are significantly different (see, for example, Fig. 8).

Recent EPR experiments show that the disorder potential of the amorphous phase leads to a stronger localization of P- and As-donor states in hydrogenated amorphous Si and Ge in comparison to the same donors in the corresponding crystalline semiconductors.[40] In a similar fashion, the potential fluctuations due to the compositional disorder in $Al_xGa_{1-x}As$ may lead to a deepening of the Si shallow hydrogenic effective-mass states. The short-range potential can mix states of different $\mathbf{k}$ vector[41] and, thus, lead to a coupling interaction between states derived from the X_x and X_y valleys or between states derived from the Γ- and X-point conduction-band minima. These intervalley (i.e., X_x-X_y or Γ-X) scattering interactions may explain the decrease in g-value anisotropy found in the $(1\bar{1}0)$ planes and the increasing linewidth of the donor resonances in the Si-doped $Al_xGa_{1-x}As$ samples as x varies from 1 to 0.5. Further theoretical work is needed to determine the strength of these interactions.

Recently, absorption and photoluminescence experiments have provided evidence of a strongly localized donor state with A_1 symmetry for Si-doped GaAs under hydrostatic pressure.[42,43] These experiments suggest that there are three different states of the same donor impurity: the hydrogenic effective-mass shallow state, "deep" A_1 state, and DX-like state. The existence of highly localized electronic states with A_1 symmetry was predicted from tight-binding approximation theories.[44] In addition, this A_1 deep donor state has *no* energy barrier for the transfer of electrons from the shallow state. Thus, the present ODMR results on the Si-doped $Al_xGa_{1-x}As$ sample with intermediate Al mole composition may reflect a contribution of these localized A_1 states to the makeup of the donor state probed. As stated in Sec. V B, an isotropic g value is usually associated with an A_1 state. In this case, the value associated with this A_1 state could be expected to be near ~ 1.95, the appropriate average g value (i.e., $\frac{1}{3}g_\parallel + \frac{2}{3}g_\perp$) derived from the single-valley g parameters found for the Si-doped AlAs sample.

Thus, the reduced g-value anisotropy observed in the $(1\bar{1}0)$ plane with decreasing x may reflect a deepening of the shallow state due to a coupling interaction that mixes the X_x and X_y valleys and/or the participation of a deep, but optically active, A_1 state.

D. Sn donors in AlAs and $Al_xGa_{1-x}As$

The results for the Sn-doped AlAs/GaAs heterostructure are quite different from the spectra observed for the Si-doped AlAs/GaAs sample. The combined observations of the luminescence-increasing resonance with g value near 2 and the isotropy of the g value with the applied field rotated in the $(1\bar{1}0)$ plane suggest that the optically active state in this sample is much deeper compared to the Si-donor state in AlAs. Again, no valley-orbit interaction is expected for the Sn dopant when it is substitutional on the Al site.[21] However, the spin-valley interaction may be important for Sn donors in AlAs due to the much larger difference in atomic mass between Sn and Al compared to that between Si and Al. This interaction may produce a coupling among the X valleys and lead to a deepening of the Sn donor state in AlAs. In addition, strong luminescence-increasing resonances with isotropic g values near 2 were observed also in the Sn-doped $Al_xGa_{1-x}As$ samples with $x=0.6$ and 0.4.

Recently, clearly resolved hyperfine splittings due to the magnetic ^{117}Sn and ^{119}Sn isotopes ($I=\frac{1}{2}$) have been observed from absorption magnetic circular dichroism (MCD) ODMR experiments[45] on a 100-μm-thick Sn-doped $Al_xGa_{1-x}As$ freestanding layer with $x=0.39$ grown by OMVPE. The strong, central single-resonance feature due to the more naturally abundant ^{118}Sn isotope ($I=0$) was found with $g=1.97\pm0.03$ and FWHM$=51\pm5$ mT. This g value is similar to the g values of the dominant features observed in the present ODMR studies on the three Sn-doped $Al_xGa_{1-x}As$ samples. The spectrum was assigned to a deep level paramagnetic state from the magnitude of the Sn hyperfine interaction term. However, it is not clear whether the dominant resonances found in the ODMR or MCD experiments arise from isolated Sn on the group-III site or from a Sn-related complex.

As noted earlier, the luminescence-increasing resonance observed from the Sn-doped AlAs layer exhibits a large anisotropy in intensity as the field is rotated from [110] to [001]. However, the intensity of the $g\sim2$ line found in the Sn-doped $Al_{0.6}Ga_{0.4}As$ sample did not exhibit a strong variation in the $(1\bar{1}0)$ plane. The behavior observed from the Sn-doped AlAs sample is very similar to the characteristics observed previously for donor centers in ODMR studies of CdS.[46] The intensity of the donor ODMR signal in the CdS samples was found to increase as the field was rotated towards the c axis of the wurtzite structure. This behavior was attributed to the dependence of the optical selection rules on the angle between the magnetic field and the crystal field along the c axis. This is due to the strong polarization parallel to the c axis of the spin of the shallow acceptor that participates in the donor-acceptor pair recombination.

VI. SUMMARY

Optically detected magnetic-resonance experiments have been performed on doped epitaxial layers of AlAs and $Al_xGa_{1-x}As$ with $x\geq0.35$. The $Al_xGa_{1-x}As$ layers were doped during growth or via implantation with Si and Sn impurity atoms from group IV and S, Se, and Te impurity atoms from group VI. The studies were carried out with the as-grown epitaxial layers on the parent (001) GaAs substrates, removed from the substrates, attached to substrates with larger lattice constants at low temperatures (for example, silica), and under applied uniaxial stresses along the $[1\bar{1}0]$ and [100] in-plane directions. Also, symmetry information was obtained from angular-rotation studies with the magnetic field rotated in the $(1\bar{1}0)$ and (001) crystal planes.

The donor state in Si-doped AlAs observed in these ODMR studies can be described by the usual hydrogenic effective-mass theory for substitutional donors on the group-III site associated with the X-point conduction-band minima. The ODMR results reveal that Si donors behave as a local probe of the strain fields in AlAs. For example, the anisotropy and splitting behavior confirms that the heteroepitaxial strain due to the mismatch of the AlAs and GaAs lattice constants at 1.6 K raises the X_z valley relative to the X_x and X_y valleys in thin layers of AlAs grown on (001) GaAs substrates. Also, these studies provide evidence for negligible valley-orbit interactions for Si donors on the group-III site in AlAs as predicted by Morgan[21] and for negligible spin-orbit coupling.

The ODMR studies on the $Al_xGa_{1-x}As$ layers doped with S, Se, and Te from group-VI provide strong evidence, particularly for samples with $x\geq0.6$, that (1) these optically active states are located on the group-V site and (2) form shallow states derived from the X-point conduction-band minima. The results can be described by the hydrogenic effective-mass theory modified by a finite valley-orbit (i.e., central cell) interaction that mixes the states derived from the X_x, X_y, and X_z valleys as predicted by Morgan.[21] This prediction was verified from the comparison between the Si-doped $Al_{0.6}Ga_{0.4}As$ sample and the $Al_{0.6}Ga_{0.4}As$ layers doped with S, Se, and Te. Analyses of the ODMR results yield valley-orbit splitting energies (i.e., chemical shifts) of ~16–20 meV for these group-VI donors.

The nature of the donor states in the Si-doped $Al_xGa_{1-x}As$/GaAs heterostructures with $x<1$ is not well understood within the virtual-crystal approximation, particularly for samples with x near 0.4. The monotonic decrease in both the g-value anisotropy and splitting with decreasing Al mole fraction observed from the angular-rotation studies in the $(1\bar{1}0)$ and (001) planes indicates a breakdown of the independent-valley model that was employed to describe the donor ground state in Si-doped AlAs. The behavior of the Si-donor resonances with decreasing x reflect more of an A_1 (singlet) character rather than a T_2 (triplet) state (however, modified by the heteroepitaxial strain) found for Si donors in AlAs. The ODMR results suggest the presence of one or more interactions (including alloy disorder) among states derived

from the X_x, X_y, and X_z valleys or perhaps a coupling of donor states derived from the X-point conduction-band minima with states derived from the Γ and/or L bands. ODMR experiments performed with externally applied uniaxial stress along the $[1\bar{1}0]$ and [100] directions on the Si-doped $Al_{0.4}Ga_{0.6}As$ sample provide evidence against the contribution of donor states derived from the L-point conduction-band minima at $x=0.4$.

The results for the Sn-doped AlAs/GaAs and Sn-doped $Al_xGa_{1-x}As$/GaAs heterostructures with $x<1$ are quite different from the spectra observed from the corresponding Si-doped samples. The Sn-doped $Al_xGa_{1-x}As$ samples with $x=0.4$, 0.6, and 1 exhibit a broad line with an isotropic g value $=2.00\pm0.02$. Recent absorption (MCD) ODMR experiments[45] on Sn-doped $Al_{0.4}Ga_{0.6}As$ provide evidence for a Sn-related paramagnetic deep level state with strong A_1 character. However it is not clear whether the dominant resonances found in the MCD and the present ODMR experiments are from isolated Sn on the group-III site or from a Sn-related defect complex. Further experiments, such as electron-nuclear double resonance (ENDOR), that can probe the local environment of the defect center can potentially address this issue.

ACKNOWLEDGMENTS

We thank M. Fatermi for the double-crystal x-ray measurements. Thanks are also due J. M. Trombetta, T. L. Reinecke, E. A. Montie, J. C. M. Henning, W. Wilkening, and U. Kaufmann for many helpful discussions and the exchange of results prior to publication. This work was supported in part by the U.S. Office of Naval Research.

*Present address: University of Wisconsin, Department of Chemical Engineering, Madison, Wisconsin 53706.

[1]For a review, see P. M. Mooney, J. Appl. Phys. **67**, R1 (1990).

[2]H. J. von Bardeleben, J. C. Bourgoin, P. Basmaji, and P. Gibart, Phys. Rev. B **40**, 5892 (1989), and private communication.

[3]P. M. Mooney, W. Wilkening, U. Kaufmann, and T. F. Kuech, Phys. Rev. B **39**, 5554 (1989).

[4]K. Khachaturyan, E. R. Weber, and M. Kaminska, Mat. Sci. Forum **38-41**, 1067 (1989).

[5]D. J. Chadi and K. J. Chang, Phys. Rev. Lett. **61**, 873 (1988).

[6]K. A. Khachaturyan, D. D. Awschalom, J. R. Rosen, and E. R. Weber, Phys. Rev. Lett. **63**, 1311 (1989).

[7]S. Wartewig, R. Böttcher, and G. Kuhn, Phys. Status Solidi B **70**, K23 (1975), and references therein.

[8]T. A. Kennedy, R. Magno, E. Glaser, and M. G. Spencer, in *Defects in Electronic Materials, Fall 1987,* edited by M. Stavola, S. J. Pearton, and G. Davies, MRS Symposia Proceedings No. 104 (Materials Research Society, Pittsburgh, 1988), p. 555.

[9]E. Glaser, T. A. Kennedy, and B. Molnar, in *Shallow Impurities in Semiconductors—1988,* Proceedings of the Third International Conference on Shallow Impurities in Semiconductors, edited by B. Monemar, IOP Conf. Proc. No. 95 (Institute of Physics, and Physical Society, Bristol, 1989), p. 233.

[10]T. A. Kennedy and E. Glaser, in *Physics of DX Centers in GaAs Alloys,* edited by J. C. Bourgoin (Sci-Tech, Brookfield, VT, 1990), p. 53.

[11]E. A. Montie and J. C. M. Henning, J. Phys. C **21**, L311 (1988).

[12]J. C. M. Henning, E. A. Montie, and J. P. M. Ansems, in *Materials Science Forum,* edited by G. Ferenczi (Trans Tech, Switzerland, 1989), Vols. 38–41, p. 1085.

[13]E. A. Montie, J. C. M. Henning, and E. C. Cosman, Phys. Rev. B **42**, 11 808 (1990).

[14]E. Glaser, T. A. Kennedy, R. S. Sillmon, and M. G. Spencer, Phys. Rev. B **40**, 3447 (1989).

[15]U. Kaufmann, W. Wilkening, P. M. Mooney, and T. F. Kuech, Phys. Rev. B **41**, 10 206 (1990).

[16]E. Glaser, T. A. Kennedy, B. Molnar, and M. Mizuta, in *Impurities, Defects, and Diffusion in Semiconductors: Bulk and Layered Structures,* edited by D. J. Wolford, J. Bernholc, and E. E. Maller, MRS Symposia Proc. No. 163 (Materials Research Society, Pittsburgh, 1990), p. 753.

[17]H. J. von Bardeleben, M. Zazoui, S. Alaya, and P. Gibart, Phys. Rev. B **42**, 1500 (1990).

[18]See, e.g., J. M. Ziman, *Models of Disorder* (Cambridge University Press, Cambridge, 1979).

[19]T. N. Theis, T. F. Kuech, L. F. Palmateer, and P. M. Mooney, in *Gallium Arsenide and Related Compounds 1984,* Proceedings of the Eleventh International Symposium on GaAs and Related Compounds, edited by B. de Cremoux, IOP Conf. Proc. No. 74 (Institute of Physics and Physical Society, Bristol, 1984), p. 241.

[20]T. Inoshita and N. Iwata, Phys. Rev. B **42**, 1296 (1990).

[21]T. N. Morgan, Phys. Rev. B **34**, 2664 (1986), and references therein.

[22]F. Mehran, T. N. Morgan, R. S. Title, and S. E. Blum, Phys. Rev. B **6**, 3917 (1972).

[23]See R. K. Watts, *Point Defects in Crystals* (Wiley, New York, 1977), p. 217, and references therein.

[24]M. Altarelli, J. Phys. Soc. Jpn. **49**, Suppl. A, 169 (1980).

[25]F. Mehran, T. N. Morgan, R. S. Title, and S. E. Blum, Solid State Commun. **11**, 661 (1972).

[26]L. M. Roth, Phys. Rev. **118**, 1534 (1960).

[27]W. Wilkening and U. Kaufmann, in *Proceedings of the 4th International Conference on Shallow Impurities in Semiconductors,* edited by G. Davies (Trans Tech, Switzerland, 1991), p. 397.

[28]S. Logothetidis, M. Alouani, M. Garriga, and M. Cardona, Phys. Rev. B **41**, 2959 (1990).

[29]S. Adachi, J. Appl. Phys. **58**, R1 (1985).

[30]G. Oelgart, R. Schwabe, M. Heider, and B. Jacobs, Semicond. Sci. Technol. **2**, 468 (1987).

[31]M. Fockele, B. K. Meyer, J. M. Spaeth, M. Heuken, and K. Heime, Phys. Rev. B **40**, 2001 (1989); T. A. Kennedy, R. Magno, and M. G. Spencer, *ibid.* **37**, 6325 (1988).

[32]H. W. van Kesteren, E. C. Cosman, P. Dawson, K. J. Moore, and C. T. Foxon, Phys. Rev. B **39**, 13 426 (1989).

[33]K. Kamigaki, H. Sakashita, H. Kato, M. Nakayama, N. Sano, and H. Terauchi, Appl. Phys. Lett. **49**, 1071 (1986).

[34]P. Lefebvre, B. Gil, H. Mathieu, and R. Planel, Phys. Rev. B **40**, 7802 (1989).

[35]R. S. Title and T. N. Morgan, Bull. Am. Phys. Soc. **15**, 267

(1970).
[36]M. Schlierkamp, R. Wille, K. Greipel, U. Rossler,W. Schlapp, and G. Weiman, Phys. Rev. B **40**, 3077 (1989).
[37]D. K. Wilson and G. Feher, Phys. Rev. **124**, 1068 (1961).
[38]T. N. Theis, in *Shallow Impurities in Semiconductors—1988,* Proceedings of Third International Conference on Shallow Impurities in Semiconductors, edited by B. Monemar, IOP Conf. Proc. No. 95 (Institute of Physics and Physical Society, Bristol, 1989), p. 307.
[39]J. E. Dmochowski, L. Dobaczewski, J. M. Langer, and W. Jantsch, Phys. Rev. B **40**, 9671 (1989).
[40]M. Stutzmann and R. A. Street, Phys. Rev. Lett. **54**, 1836 (1985).
[41]M. V. Klein, M. D. Sturge, and E. Cohen, Phys. Rev. B **25**, 4331 (1982).
[42]J. E. Dmochowski, P. D. Wang, and R. A. Stradling, in *Proceedings of the 20th International Conference on the Physics of Semiconductors,* edited by E. M. Anastassakis, and J. D. Joannopoulos (World Scientific, Singapore, 1990), p. 658.
[43]X. Liu, L. Samuelson, M.-E. Pistol, M. Gerling, and S. Nilsson, Phys. Rev. B **42**, 11 791 (1990).
[44]H. P. Hjalmarson, P. Vogl, D. J. Wolford, and J. D. Dow, Phys. Rev. Lett. **44**, 810 (1980).
[45]M. Fockele, J.-M. Spaeth, and P. Gibart, in *Proceedings of the 20th International Conference on the Physics of Semiconductors* (Ref. 42), p. 517.
[46]J. L. Patel, J. E. Nicholls, and J. J. Davies, J. Phys. C **14**, 1339 (1981).